Thermal Effects of CNTs Nanoliquid Film Flow During Spin Coating

Swatilekha Nag and Susanta Maity

Nomenclature

Bi	Biot number
C_0	Constant
C_1	Constant
C_p	Heat capacity at constant pressure (J/kg K)
Fr	Froude number
h	Film thickness (m)
h_0	Initial film thickness (m)
k	Thermal conductivity (W/m K)
p	Pressure of nanoliquid (Pa)
Pr	Prandtl number
Re	Reynolds number
t	Rotational time (s)
t_c	Characteristic time (s)
T	Nanoliquid temperature (K)
T_g	Temperature in gas phase (K)
T_0	Room temperature (K)
We	Weber number

Greek Symbols

α	Thermocapillary parameter
β	Heat transfer coefficient
ϵ	Aspect ratio
μ	Dynamic viscosity (kg/m s)

S. Nag · S. Maity (✉)
Department of Basic and Applied Science, National Institute of Technology, Arunachal Pradesh, India
e-mail: susanta@nitap.ac.in

© The Author(s), under exclusive license to Springer Nature Singapore Pte Ltd. 2022

P. Mahanta et al. (eds.), *Advances in Thermofluids and Renewable Energy*, Lecture Notes in Mechanical Engineering, https://doi.org/10.1007/978-981-16-3497-0_11

ν	Kinematic viscosity (m^2/s)
Ω	Angular velocity of the disk (s^{-1})
ϕ	Nanoparticle volume fraction
ϕ_1, ϕ_2	Dimensionless constant
ψ_1	Radial velocity component (m/s)
ψ_2	Cross-radial velocity component (m/s)
ψ_3	Velocity component perpendicular to disk (m/s)
ρ	Density (kg/m^3)
σ	Surface tension (kg/s^2)
σ_0	Surface tension at initial time (kg/s^2)

Subscript

bl	Base liquid
nl	Nanoliquid
CNTs	Nanoparticle

1 Introduction

The spin coating is a process by which a very thin uniform film layer (layers of paint, polymer, lacquer, etc.) is developed over the surface of a horizontal rotating substrate/disk with the help of centrifugal force. The thin film development over a spinning disk is very important in microelectronic industries. Nowadays, we are living in the electronic age and using electronic gadgets frequently in our daily life. Many of these gadgets have the hard disk, screen, electronic circuit, etc. In manufacturing of these gadgets, the coating is required in many intermediate steps. This technique is also broadly used in magnetic disk for data storage, small-scale gadget industry to fabricate the incorporated circuits, optical mirrors and color television screens, etc. The investigation of thin Newtonian liquid film over a spinning disk was first theoretically initiated by Emslie et al. [1]. Acrivos et al. [2] and Jenekhe and Schuldt [3] extended the analysis to think about the stream of a non-Newtonian power-law liquid film flow over a spinning disk. In spin coating process, the effect of solvent evaporation was first introduced by Myerhofer [5]. Middleman [6] examined the impact of air shear at the liquid–air interface on the development of liquid film through the spin coating process. Higgins [4] analyzed the unsteady liquid film flow on a rotating disk by match asymptotic methods by considering full set of momentum equations. Dandapat and Ray [7, 8] explored the influence of heating/cooling of the disk surface on thin liquid film development over a spinning disk. Dandapat et al. [9] studied the two-layer thin film flow on a rough spinning disk in the presence of air shear at the liquid–air interface. Dandapat and Maity [10] investigated the impacts of external air flow on a thin film flow over a rotating annular disk with the deformable

free surface. Dandapat et al. [11] analyzed the thermal effects of thin liquid film flow on a spinning disk.

In recent year, nanofluid has gained huge attentions of the researchers due to its increased heat transfer performance. Nanofluid is the colloidal suspension of nanometer size metallic or nonmetallic particles (1–100 nm) with the conventional heat transfer fluids like water, ethylene glycol, engine oil, etc. In the presence of tiny-sized particles, the thermal conductivity of the conventional fluids enhances anomalously. The nanofluid was first discovered by Choi [12] and showed the anomalous increase of thermal conductivity of the conventional fluids. Buongiorno [13] investigated the laminar flow of nanofluids by taking effects of thermophoresis and Brownian motion. Carbon nanotubes-based nanofluids (CNTs) are also very important due to its unique properties such as high electrical conductivity, high mechanical strength, and high thermal conductivity. Akbar and Butt [14] considered the peristaltic flow of CNTs suspended nanofluid over a curved channel. Hussanan et al. [15] studied the magnetohydrodynamic flow of CNTs nanofluid flow on a stretching sheet. Recently, Maity [16] investigated water-based thin nanoliquid film development during spin coating process.

In this article, we have modeled the thin CNTs nanoliquid film development over a spinning horizontal disk. It is assumed that the nanoliquid film is deformable. The effects of both single-walled carbon nanotubes (SWCNTs) and multi-walled carbon nanotubes (MWCNTs) are considered for investigation.

2 Formulation of the Problem

We have considered an axisymmetric, viscous, incompressible water-based CNTs nanoliquid film flow on a rotating disk. We choose the cylindrical polar coordinate system with the origin at center of the disk, and the z-axis is vertically upward. Initially, the disk is at rest at time $t = 0$ and it starts to rotate with angular velocity Ω about the z-axis. At the begin, the framework is at room temperature T_0. Let (ψ_1, ψ_2, ψ_3) and T be the velocity components along (r, θ, z) direction and temperature of the nanoliquid, respectively. The axisymmetric equation of continuity and momentum and energy equations can be written as:

$$\frac{\partial \psi_1}{\partial r} + \frac{\psi_1}{r} + \frac{\partial \psi_3}{\partial z} = 0, \tag{1}$$

$$\begin{aligned} \rho_{\mathrm{nl}}\left[\frac{\partial \psi_1}{\partial t} + \psi_1 \frac{\partial \psi_1}{\partial r} + \psi_3 \frac{\partial \psi_1}{\partial z} - \frac{{\psi_2}^2}{r}\right] &= -\frac{\partial p}{\partial r} \\ +\mu_{\mathrm{nl}}\left[\frac{\partial^2 \psi_1}{\partial r^2} + \frac{\partial}{\partial r}\left(\frac{\psi_1}{r}\right) + \frac{\partial^2 \psi_1}{\partial z^2}\right], \end{aligned} \tag{2}$$

$$\rho_{\mathrm{nl}}\left[\frac{\partial\psi_2}{\partial t}+\psi_1\frac{\partial\psi_2}{\partial r}+\psi_3\frac{\partial\psi_2}{\partial z}+\frac{\psi_1\psi_2}{r}\right]= \mu_{\mathrm{nl}}\left[\frac{\partial^2\psi_2}{\partial r^2}+\frac{\partial}{\partial r}\left(\frac{\psi_2}{r}\right)+\frac{\partial^2\psi_2}{\partial z^2}\right], \tag{3}$$

$$\rho_{\mathrm{nl}}\left[\frac{\partial\psi_3}{\partial t}+\psi_1\frac{\partial\psi_3}{\partial r}+\psi_3\frac{\partial\psi_3}{\partial z}\right]=-\frac{\partial p}{\partial z} +\mu_{\mathrm{nl}}\left[\frac{\partial^2\psi_3}{\partial r^2}+\frac{1}{r}\frac{\partial\psi_3}{\partial r}+\frac{\partial^2\psi_3}{\partial z^2}\right], \tag{4}$$

$$\left(\rho C_p\right)_{\mathrm{nl}}\left[\frac{\partial T}{\partial t}+\psi_1\frac{\partial T}{\partial r}+\psi_3\frac{\partial T}{\partial z}\right]=k_{\mathrm{nl}}\left[\frac{\partial^2 T}{\partial r^2} +\frac{1}{r}\frac{\partial T}{\partial r}+\frac{\partial^2 T}{\partial z^2}\right], \tag{5}$$

where p, ρ_{nl}, μ_{nl}, $(\rho C_p)_{\mathrm{nl}}$, and k_{nl} are, respectively, the pressure, density, dynamic viscosity, heat capacity, and thermal conductivity of the water-based CNTs nanoliquid. These are defined as follows:

$$\rho_{\mathrm{nl}}=(1-\phi)\rho_{\mathrm{bl}}+\phi\rho_{\mathrm{CNTs}}, \tag{6}$$

$$\mu_{\mathrm{nl}}=\frac{\mu_{\mathrm{bl}}}{(1-\phi)^{\frac{5}{2}}}, \tag{7}$$

$$(\rho C_p)_{\mathrm{nl}}=(1-\phi)(\rho C_p)_{\mathrm{bl}}+\phi(\rho C_p)_{\mathrm{CNTs}}, \tag{8}$$

$$k_{\mathrm{CNTs}}=k_{\mathrm{bl}}\left(\frac{(1-\phi)+\frac{2\phi k_{\mathrm{CNTs}}}{k_{\mathrm{CNTs}}-k_{\mathrm{bl}}}\log\left(\frac{k_{\mathrm{CNTs}}+k_{\mathrm{bl}}}{2k_{\mathrm{bl}}}\right)}{(1-\phi)+\frac{2\phi k_{\mathrm{bl}}}{k_{\mathrm{CNTs}}-k_{\mathrm{bl}}}\log\left(\frac{k_{\mathrm{CNTs}}+k_{\mathrm{bl}}}{2k_{\mathrm{bl}}}\right)}\right), \tag{9}$$

where suffixes *bl* and CNTs stand for the properties of the base liquid and carbon nanotubes, respectively, and ϕ is the volume fraction of CNTs.

The corresponding boundary and initial conditions are given below: at the surface of the rotating disk ($z=0$),

$$\psi_1 = 0, \psi_2 = r\Omega, \psi_3 = 0, T = \theta(r), \tag{10}$$

at the liquid–air interface $z = h(r, t)$,

$$\begin{aligned} &-p + \frac{2\mu_{\mathrm{nl}}}{1 + {h_r}^2}[{h_r}^2\psi_{1_r} - h_r(\psi_{1_z} + \psi_{3_r}) + \psi_{3_z}] \\ &= \frac{\sigma}{r}\left[\frac{h_r(1 + {h_r}^2) + rh_{\mathrm{rr}}}{(1 + {h_r}^2)^{3/2}}\right], \end{aligned} \tag{11}$$

$$\begin{aligned} &\frac{\mu_{\mathrm{nl}}}{(1 + {h_r}^2)^{1/2}}[2h_r(\psi_{1_r} - \psi_{3_z}) + ({h_r}^2 - 1) \\ &(\psi_{3_r} + \psi_{1_z})] = -(\sigma_r + h_r\sigma_z), \end{aligned} \tag{12}$$

$$\psi_{2z} - rh_r\left(\frac{\psi_2}{r}\right)_r = 0, \tag{13}$$

$$h_t + \psi_1 h_r = \psi_3, \tag{14}$$

$$-k_{\mathrm{nl}}[T_z - h_r T_r] = \beta(T - T_0)\sqrt{1 + {h_r}^2}, \tag{15}$$

the initial condition at time $t = 0$,

$$\psi_1 = 0, \psi_2 = 0, \psi_3 = 0, h(r, 0) = \delta(r), T = T_0, \tag{16}$$

where σ is the surface tension which varies linearly with the temperature T as $\sigma = \sigma_0 - \gamma(T - T_0)$ and γ is a positive constant. β is the heat transfer coefficient. The temperature depended physical properties of the water and CNTs are given in Table 1.

Table 1 Physical properties of base liquids and CNTs (see Hussanan et al. [15], Krishanan et al. [17])

	$\rho\left(\frac{\mathrm{kg}}{\mathrm{m}^3}\right)$	$C_p\left(\frac{\mathrm{J}}{\mathrm{kgK}}\right)$	$k\left(\frac{\mathrm{W}}{\mathrm{mK}}\right)$
Water	997.1	4179	0.613
SWCNT	2600	425	6600
MWCNT	1600	796	3000

To find the non-dimensional form of the governing set of Eqs. (1)–(5), the following dimensionless variables are introduced as

$$\hat{t} = \frac{t}{t_c}, \hat{r} = \frac{r}{R}, \hat{z} = \frac{z}{h_0}, \hat{\delta} = \frac{\delta}{h_0}, \hat{h} = \frac{h}{h_0},$$
$$\hat{\psi}_1 = \frac{\psi_1}{U_0}, \hat{\psi}_2 = \frac{\psi_2\sqrt{\epsilon \mathrm{Re}}}{U_0}, \hat{\psi}_3 = \frac{\psi_3}{\epsilon U_0}, \hat{p} = \frac{{h_0}^2 t_c}{\nu_{bl} R^2 \rho_{bl}} p,$$
$$U_0 = \frac{R}{t_c}, \hat{T} = \frac{T - T_0}{T_{d_0} - T_0}, t_c = \frac{\nu_{bl}}{(\Omega h_0)^2},$$

where $\mathrm{Re} = U_0 h_0/\nu_{bl}$ is the Reynolds number, h_0 is the average value of initial film profile, $\epsilon = h_0/R(\ll 1)$ is the aspect ratio, R is the radius of the disk, and T_{d0} is imposed temperature at the center of the disk. Finally, we get the non-dimensional governing set of equations as:

$$\frac{\partial \hat{\psi}_1}{\partial \hat{r}} + \frac{\hat{\psi}_1}{\hat{r}} + \frac{\partial \hat{\psi}_3}{\partial \hat{z}} = 0, \tag{17}$$

$$\epsilon \mathrm{Re} \phi_1 \left[\frac{\partial \hat{\psi}_1}{\partial \hat{t}} + \hat{\psi}_1 \frac{\partial \hat{\psi}_1}{\partial \hat{r}} + \hat{\psi}_3 \frac{\partial \hat{\psi}_1}{\partial \hat{z}} \right] = -(1-\phi)^{2.5} \frac{\partial \hat{p}}{\partial \hat{r}}$$
$$+ \phi_1 \frac{{\hat{\psi}_2}^2}{\hat{r}} + \epsilon^2 \left[\frac{\partial^2 \hat{\psi}_1}{\partial \hat{r}^2} + \left(\frac{\hat{\psi}_1}{\hat{r}} \right)_{\hat{r}} \right] + \frac{\partial^2 \hat{\psi}_1}{\partial \hat{z}^2}, \tag{18}$$

$$\epsilon \mathrm{Re} \phi_1 \left[\frac{\partial \hat{\psi}_2}{\partial \hat{t}} + \hat{\psi}_1 \frac{\partial \hat{\psi}_2}{\partial \hat{r}} + \hat{\psi}_3 \frac{\partial \hat{\psi}_2}{\partial \hat{z}} + \frac{\hat{\psi}_1 \hat{\psi}_2}{\hat{r}} \right] =$$
$$\left[\epsilon^2 \left(\frac{\partial^2 \hat{\psi}_2}{\partial \hat{r}^2} + \left(\frac{\hat{\psi}_2}{\hat{r}} \right)_{\hat{r}} \right) + \frac{\partial^2 \hat{\psi}_2}{\partial \hat{z}^2} \right], \tag{19}$$

$$\epsilon^3 \mathrm{Re} \phi_1 \left[\frac{\partial \hat{\psi}_3}{\partial \hat{t}} + \hat{\psi}_1 \frac{\partial \hat{\psi}_3}{\partial \hat{r}} + \hat{\psi}_3 \frac{\partial \hat{\psi}_3}{\partial \hat{z}} \right] = -(1-\phi)^{2.5} \frac{\partial \hat{p}}{\partial \hat{z}}$$
$$+ \epsilon^2 \left[\epsilon^2 \left(\frac{\partial^2 \hat{w}}{\partial \hat{r}^2} + \frac{1}{\hat{r}} \frac{\partial \hat{w}}{\partial \hat{r}} \right) + \frac{\partial^2 \hat{w}}{\partial \hat{z}^2} \right] - \epsilon \mathrm{Fr} \phi_1, \tag{20}$$

$$\epsilon \mathrm{Re}\,\mathrm{Pr}\phi_2\left[\frac{\partial \hat{T}}{\partial \hat{t}}+\hat{\psi}_1\frac{\partial \hat{T}}{\partial \hat{r}}+\hat{\psi}_3\frac{\partial \hat{T}}{\partial \hat{z}}\right]=$$
$$\frac{k_{\mathrm{nf}}}{k_f}\left[\epsilon^2\left(\frac{\partial^2 \hat{T}}{\partial \hat{r}^2}+\frac{1}{\hat{r}}\frac{\partial \hat{T}}{\partial \hat{r}}\right)+\frac{\partial^2 \hat{T}}{\partial \hat{z}^2}\right], \tag{21}$$

where $\mathrm{Fr}=gh_0^2/(U_0\nu_{\mathrm{bl}})$ is the modified Froude number, $\mathrm{Pr}=\frac{\nu_f}{\alpha_f}$ is the Prandtl number, $\phi_1=(1-\phi)^{2.5}[(1-\phi)+\phi\frac{\rho_s}{\rho_f}]$, $\phi_2=(1-\phi)+\phi\frac{(\rho c_p)_s}{(\rho c_p)_f}$.

The non-dimensional boundary and initial conditions are given below:
at $\hat{z}=0$,

$$\hat{\psi}_1=0,\ \hat{\psi}_2=\hat{r},\ \hat{\psi}_3=0,\ \hat{T}=\hat{\theta}(\hat{r}), \tag{22}$$

at $\hat{z}=\hat{h}(\hat{r},\hat{t})$,

$$-p+\frac{2\epsilon^2(1-\phi)^{2.5}}{(1+\epsilon^2\hat{h}_{\hat{r}}^2)}[\epsilon^2\hat{h}_{\hat{r}}\hat{\psi}_{1\hat{r}}-\hat{h}_{\hat{r}}(\hat{\psi}_{1\hat{z}}+\epsilon^2\hat{\psi}_{3\hat{r}})$$
$$+\hat{\psi}_{3\hat{z}}]=\frac{\epsilon}{\hat{r}}[\mathrm{We}-\epsilon^2\alpha\hat{T}][\frac{\hat{h}_{\hat{r}}(1+\epsilon^2\hat{h}_{\hat{r}}^2)+\hat{r}\hat{h}_{\hat{r}\hat{r}}}{(1+\epsilon^2\hat{h}_{\hat{r}}^2)^{3/2}}], \tag{23}$$

$$2\epsilon^2\hat{h}_{\hat{r}}(\hat{\psi}_{3\hat{z}}-\hat{\psi}_{1\hat{r}})+(1-\epsilon^2\hat{h}_{\hat{r}}^2)(\epsilon^2\hat{\psi}_{3\hat{r}}+\hat{\psi}_{1\hat{z}})$$
$$=-(1-\phi)^{2.5}\epsilon\alpha(\hat{T}_{\hat{r}}+\hat{h}_{\hat{r}}\hat{T}_{\hat{z}})\sqrt{1+\epsilon^2\hat{h}_{\hat{r}}^2}, \tag{24}$$

$$\hat{\psi}_{2\hat{z}}-\epsilon^2\hat{r}\hat{h}_{\hat{r}}\left(\frac{\hat{\psi}_2}{\hat{r}}\right)_{\hat{r}}=0, \tag{25}$$

$$\frac{k_{\mathrm{nf}}}{k_f}(\hat{T}_{\hat{z}}-\epsilon^2\hat{h}_{\hat{r}}\hat{T}_{\hat{r}})=-Bi\hat{T}\sqrt{1+\epsilon^2\hat{h}_{\hat{r}}^2}, \tag{26}$$

$$-\frac{\partial \hat{h}}{\partial \hat{t}}-\hat{\psi}_1\frac{\partial \hat{h}}{\partial \hat{r}}+\hat{\psi}_3=0, \tag{27}$$

at $\hat{t} = 0$,

$$\hat{\psi_1} = 0, \hat{\psi_2} = 0, \hat{\psi_3} = 0, \hat{h} = \hat{\delta}(\hat{r}), \hat{T} = \hat{\theta}(\hat{r}), \tag{28}$$

where $\mathrm{We} = \epsilon^2\sigma_0/(\nu_{\mathrm{bl}}U_0)$ is the Weber number, $\alpha = \gamma(T_{d_0} - T_0)/(\nu_{\mathrm{bl}}U_0)$ is the thermocapillary parameter, and $\mathrm{Bi} = \beta h_0/k_{\mathrm{bl}}$ is the Biot number.

3 Asymptotic Solution

From this section onward, we have dropped the hat over the dimensionless variables for simplicity. To find the analytical solution of the coupled nonlinear system of partial differential Eqs. (17)–(21), we expanded the dependent variables in power of ϵ as

$$\begin{aligned}(\psi_1, \psi_2, \psi_3, p) &= (\psi_{10}, \psi_{20}, \psi_{30}, p_0)\\ &+\epsilon(\psi_{11}, \psi_{21}, \psi_{31}, p_1) + O(\epsilon^2),\end{aligned} \tag{29}$$

We substituted Eq. (29) upon guiding Eqs. (17)–(21) and the boundary conditions (22)–(26) and compared the coefficients of like order term of ϵ from both sides. We have obtained set of partial differential equations and solved these equations up to the first order of ϵ as

$$\begin{aligned}\psi_1 = {} & \phi_1(h - \frac{z}{2})rz + \epsilon \mathrm{Re}{\phi_1}^2 r\Bigg[h_t\left(\frac{z^3}{6} - \frac{h^2 z}{2}\right)\\ & +\phi_1\left(\frac{z^6}{360} - \frac{hz^5}{60} + \frac{2\,h^3 z^3}{9} - \frac{3\,h^5 z}{5} + \frac{rhh_r}{6}\left(\frac{z^4}{4} - h^3 z\right)\right)\Bigg]\\ & +\epsilon\left[\mathrm{Fr}h_r\phi_1 - \mathrm{We}(1-\phi)^{2.5}\left(\frac{1}{r}(rh_r)_r\right)_r\right]\left(\frac{z^2}{2} - hz\right)\\ & +\epsilon K\alpha(1-\phi)^{2.5}\left(\frac{\theta}{(K + Bih)}\right)_r z,\end{aligned} \tag{30}$$

$$\psi_2 = r + \epsilon 2\mathrm{Re}{\phi_1}^2 r\left(\frac{hz^3}{6} - \frac{z^4}{24} - \frac{h^3 z}{3}\right), \tag{31}$$

$$\psi_3 = \phi_1\left(\frac{z^3}{3} - hz^2\right) - \frac{\phi_1 r h_r z^2}{2} + \epsilon \mathrm{Re}{\phi_1}^2\Bigg[\left(h_t + \frac{rh_{rt}}{2}\right)$$
$$\times\left(\frac{h^2z^2}{2} - \frac{z^4}{12}\right) + \frac{rhh_rh_t}{2} + \phi_1\Bigg[\frac{-z^7}{1260} + \frac{hz^6}{180} + \frac{rh_rz^6}{360}$$
$$-\frac{rhh_rz^5}{40} - \frac{r^2h_r^2z^5}{120} - \frac{r^2hh_{rr}z^5}{120} - \frac{h^5z^4}{9} - \frac{rh^2h^rz^4}{6}$$
$$+\frac{3}{5}h^5z^2 + \frac{7}{4}rh^4h_rz^2 + \frac{r^2h_r^2h^3z^2}{3} + \frac{r^2h^4h_{rr}z^2}{12}\Bigg]\Bigg]$$
$$-\frac{\epsilon}{r}\Bigg[\mathrm{Fr}\phi_1(rh_r)_r - \mathrm{We}(1-\phi)^{2.5}\left\{r\left(\frac{1}{r}(rh_r)\right)_r\right\}_r\Bigg]$$
$$\times\left(\frac{z^3}{6} - \frac{hz^2}{2}\right) + \epsilon\Bigg[\mathrm{Fr}\phi_1h_r - \mathrm{We}(1-\phi)^{2.5}\left(\frac{1}{r}(rh_r)_r\right)_r\Bigg]$$
$$\times\frac{h_rz^2}{2} - \epsilon K\alpha(1-\phi)^{2.5}\frac{1}{r}\Bigg[r\left(\frac{\theta}{K+\mathrm{Bi}h}\right)_r\Bigg]_r\frac{z^2}{2}, \tag{32}$$

$$T = \frac{K+\mathrm{Bi}(h-z)}{K+\mathrm{Bi}h}\theta(r) + \epsilon\left(\frac{\mathrm{Re\,Pr}\phi_2}{K}\right)\Bigg[\frac{\mathrm{Bi}^2h_t\theta}{(K+\mathrm{Bi}h)^2}$$
$$\times\left(\frac{z^3}{6} - \frac{h^2}{6}\left(\frac{3K+\mathrm{Bi}h}{K+\mathrm{Bi}h}\right)z\right) + r\phi_1\theta_r\left(\frac{hz^3}{6} - \frac{z^4}{24}\right.$$
$$-\frac{h^3}{24}\left(\frac{8K+3\mathrm{Bi}h}{K+\mathrm{Bi}h}\right)z\Bigg) - r\phi_1\mathrm{Bi}\left(\frac{\theta}{K+\mathrm{Bi}h}\right)_r\left(\frac{hz^4}{12}\right.$$
$$-\frac{z^5}{40} - \frac{h^4}{120}\left(\frac{25K+7\mathrm{Bi}h}{K+\mathrm{Bi}h}\right)z\Bigg) - \frac{\mathrm{Bi}\theta\phi_1}{K+\mathrm{Bi}h}\left(\frac{z^5}{60}\right.$$
$$-\frac{hz^4}{12} - \frac{h^4}{60}\left(\frac{15K+4\mathrm{Bi}h}{K+Bih}\right)z\Bigg) + \frac{1}{24}\phi_1\mathrm{Bi}$$
$$\times\left(\frac{rh_r\theta}{K+\mathrm{Bi}h}\right)\left(z^4 - h^3\left(\frac{4K+\mathrm{Bi}h}{K+\mathrm{Bi}h}\right)z\right)\Bigg], \tag{33}$$

where $K = \frac{k_{\mathrm{nf}}}{k_{\mathrm{bl}}}$. It is to be mentioned here that the solutions given by Eqs. (30)–(33) do not satisfy the initial condition (28). The film evolution equation is derived by integrating the kinematic condition (27) with respect to z as

$$h_t + \frac{1}{r}\Bigg[\frac{\phi_1r^2h^3}{3} - \epsilon\mathrm{Re}{\phi_1}^2r^2\left(\frac{5}{24}h_th^4 + \phi_1\left(\frac{311}{1260}h^7\right.\right.$$
$$\left.\left.+\frac{3}{40}rh^6h_r\right)\right) - \frac{\epsilon rh^3}{3}\left\{Fr\phi_1h_r - We(1-\phi)^{2.5}\left(\frac{1}{r}(rh_r)_r\right)_r\right\}$$
$$+\frac{\epsilon K\alpha r}{2}(1-\phi)^{2.5}\left(\frac{\theta}{k+Bih}\right)_rh^2\Bigg]_r = 0. \tag{34}$$

To find the solution of Eq. (34), we expanded $h(r, t)$ by following the asymptotic procedure (29). Finally, collecting the coefficients of different powers of ϵ in Eq. (34) we get Eq. (35) for coefficient of ϵ^0 as

$$h_{0t} + \phi_1 r {h_0}^2 h_{0r} = -\frac{2}{3}\phi_1 {h_0}^3, \tag{35}$$

while coefficient of ϵ^1 gives Eq. (36).

$$\begin{aligned} h_{1t} + \phi_1 r {h_0}^2 h_{1r} &= -2\phi_1 ({h_0}^2 + r {h_0}^2 h_{0r} h_1) \\ &-\frac{1}{r}[\mathrm{Re}{\phi_1}^2 r^2 (-\frac{5}{24} h_{0t} {h_0}^4 + \phi_1 (-\frac{311}{1260} {h_0}^7 \\ &-\frac{3}{40} r {h_0}^6 h_{0r})) - \frac{1}{3} Fr \phi_1 r h_{0r} {h_0}^3 + \frac{1}{3} We (1-\phi)^{2.5} r {h_0}^3 \\ &\times \left(\frac{1}{r}(r h_{0r})_r\right)_r + k\alpha r (1-\phi)^{2.5} \left(\frac{\theta}{k + Bi h_0}\right)_r \frac{{h_0}^2}{2}]_r. \end{aligned} \tag{36}$$

It is followed from Eq. (35) that

$$\frac{\mathrm{d}}{\mathrm{d}t} h_0(r(t), t) = -\frac{2}{3}\phi_1 {h_0}^3 (r(t), t), \tag{37}$$

along the characteristics curve $r(t)$ satisfying

$$\frac{\mathrm{d}}{\mathrm{d}t} r(t) = \phi_1 r(t) {h_0}^2 (r(t), t). \tag{38}$$

Integrating above two equations, we get Eqs. (39) and (40), respectively, as

$$h_0(r(t), t) = C_0 \chi^{-1/2}, \tag{39}$$

$$r(t) = C_1 \chi^{\frac{3}{4}}, \tag{40}$$

where $\chi = 1 + (4/3)\phi_1 {C_0}^2 t$. It also follows from Eqs. (39) and (40) that

$$r(t) {h_0}^{3/2} (r(t), t) = {C_0}^{3/2} C_1 = \text{Constant}. \tag{41}$$

Solution of Eq. (36) along the characteristic curve (40) is obtained as

$$h_1(r(t),t) = \frac{K\alpha}{2}(1-\phi)^{2.5}\phi^{-1}{C_1}^{-1}(\theta_r\zeta^{-1}\chi^{-3/4} + \frac{2}{3}\theta(r)\mathrm{Bi}C_0{C_1}^{-1}\zeta^{-2}\chi^{-2}) + \frac{62}{315}\mathrm{Re}{\phi_1}^2{C_0}^5\chi^{-5/2} - \frac{2}{9}\mathrm{Fr}{C_0}^2{C_1}^{-2}\chi^{-5/2} + \frac{32}{81}\mathrm{We}{\phi_1}^{-1}(1-\phi)^{2.5}{C_0}^2{C_1}^{-4}\chi^{-4} + C_2\chi^{-1/2}, \tag{42}$$

where $\zeta = K + \mathrm{Bi}C_0\chi^{-1/2}$.

It is to be mentioned here that the above solutions do not satisfy the initial condition and these solutions are known as the longtime solution. To find the solutions that satisfy the initial condition (known as short-time solution), we have stretched the time coordinate as $\tau = t/\epsilon$ and keeping other variables same as before. Following the asymptotic expansion (29), we have obtained the short-time film thickness that satisfies the initial condition.

Now, both the solutions are matched by the following Van Dyke [18] matching principle under the assumption that flow is continuous from the start of the spinning of the disk to all succeeding time as

$$\lim_{\tau\to\infty}\overline{h}(r,\tau) = \lim_{t\to 0}h(r,t), \tag{43}$$

where $\overline{h}(r,\tau)$ is the short-time film thickness.

We have obtained the integrating constants by using equation (43) in the expression of film thickness in both the timescales as $C_1 = r(0) = \xi(\text{say})$, $C_0 = h_0(\xi,0) = \delta(\xi)$ and

$$C_2 = -\frac{K\alpha}{2}(1-\phi)^{2.5}\phi^{-1}\xi^{-1}(\theta_\xi{\zeta_0}^{-1} + \frac{2}{3}\theta(\xi)\mathrm{Bi}\delta(\xi)\xi^{-1}{\zeta_0}^{-2}) + \frac{2}{9}\mathrm{Fr}\xi^{-2}\delta(\xi)^2 - \frac{32}{81}\mathrm{We}(1-\phi)^{2.5}\phi^{-1}\xi^{-4}\delta(\xi)^2 + 0.462594\mathrm{Re}\phi_1^2\delta^5 + 1.83188\mathrm{Re}\phi_1^2\xi\delta^4\delta_\xi, \tag{44}$$

where $\zeta_0 = 1 + Bi\delta(\xi)$. The composite film thickness that is valid for all timescales is given by

$$h^c(r,t) = \overline{h}(r,t/\epsilon) + h(r,t) - h_{\mathrm{com}}(r,t), \tag{45}$$

where $h_{\mathrm{com}}(r,t)$ is the common solution.

4 Results and Discussion

In this paper, we have analyzed the development of water-based SWCNTs and MWCNTs nanoliquid film during the spin coating process. The analytical expression for the velocity, temperature field, and film thickness is obtained by the perturbation technique. The film height is computed numerically by using the initial non-uniform film profile and disk temperature distribution, respectively, as $\delta(r) = 0.47(r + 0.1)^2 e^{-r^{0.76}}$ and $\theta(r) = e^{-r^2}$. Figure 1 depicts the variation of the composite film thickness h^c with time t for different values of ϕ with SWCNTs nanoliquid, and it is observed from the figure that the film thinning rate diminishes for the increasing values of ϕ. Due to addition of the SWCNTs on the base liquid water, the viscosity of the water increases.

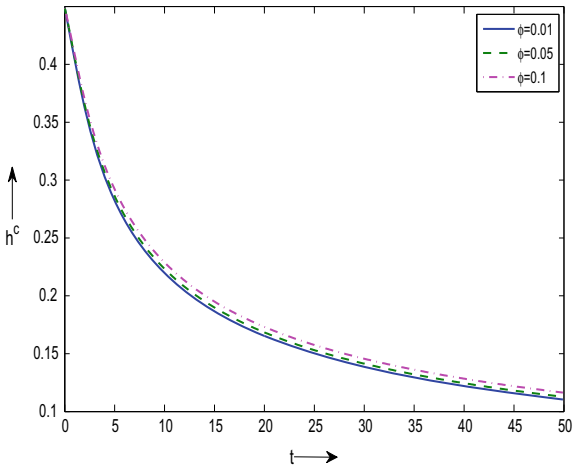

Fig. 1 Variation of film thickness h^c with time t for water-based SWCNTs nanoliquids with different values of ϕ. Here, Re $= 1.0$, Fr $= 0.1$, We $= 0.1$, $\epsilon = 0.01$, $\alpha = 0.1$, Bi $= 0.1$, $r = 4$, $\delta(r) = 0.47(r + 0.1)^2 e^{-r^{0.76}}$, $\theta(r) = e^{-r^2}$

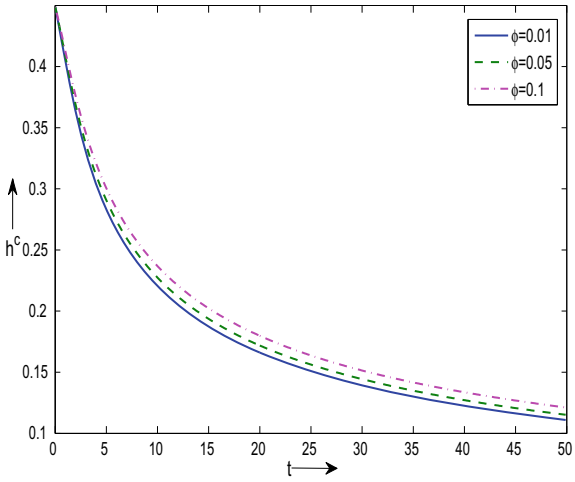

Fig. 2 Variation of film thickness h^c with time t for water-based MWCNTs nanoliquids with different values of ϕ. Here, Re $= 1.0$, Fr $= 0.1$, We $= 0.1$, $\epsilon = 0.01$, $\alpha = 0.1$, Bi $= 0.1$, $r = 4$, $\delta(r) = 0.47(r + 0.1)^2 e^{-r^{0.76}}$, $\theta(r) = e^{-r^2}$

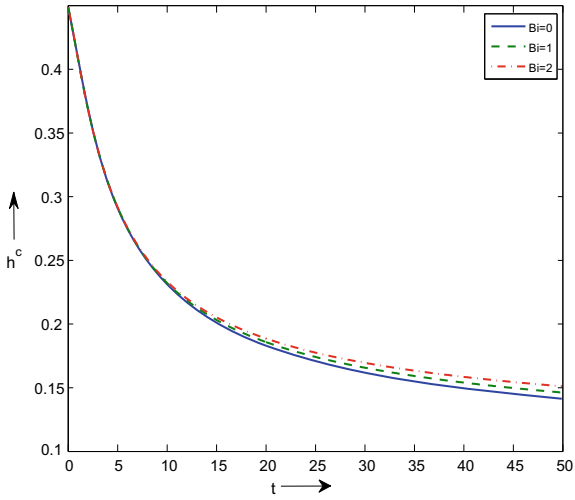

Fig. 3 Variation of film thickness h^c with time t for water-based MWCNTs nanoliquids with different values of Biot number Bi. Here, Re $= 1.0$, Fr $= 0.1$, We $= 0.1$, $\epsilon = 0.1$, $\alpha = 1$, $\phi = 0.05$, $r = 4$, $\delta(r) = 0.47(r + 0.1)^2 e^{-r^{0.76}}$, $\theta(r) = e^{-r^2}$

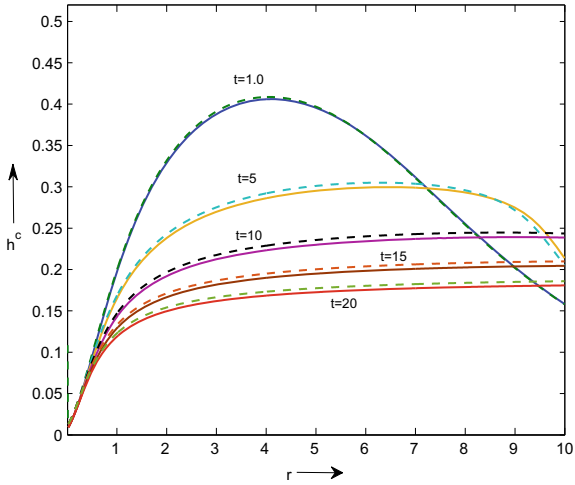

Fig. 4 Variation of film thickness h^c with r for water-based SWCNTs nanoliquids with different ϕ and t. Here, continuous line for $\phi = 0.05$ and dashed line for $\phi = 0.1$ when $Re = 1.0$, Fr $= 0.1$, We $= 0.1$, $\epsilon = 0.01$, $\alpha = 0.1$, Bi $= 0.1$, $\delta(r) = 0.47(r + 0.1)^2 e^{-r^{0.76}}$, $\theta(r) = e^{-r^2}$

As a result, the radial velocity decreases for higher values of ϕ and the film thinning rate reduces. In Fig. 2, we have plotted the variation of h^c with time t for different ϕ and MWCNTs nanoliquid. It is found the rate of film thinning decreases with rising values of ϕ.

The effects of the Biot number Bi on the film thinning process are presented in Fig. 3 for MWCNTs nanoliquid. It is clear from the figure that the rate of film thinning decreases for rising values of Bi. In general, the Biot number represents the amount of heat transfer from the SWCNTs nanoliquid to the surrounding fluid medium in comparison with heat transfer within the nanoliquid. For this reason, the thermocapillary action diminishes and the film thinning rate diminishes for larger

Biot number Bi. In Fig. 4, the chronological development of composite film thickness h^c with r is shown for different ϕ and t in SWCNTs nanoliquid. It is evident from the figure that the film thickness becomes thinner as time increases. It is also clear that the initial non-uniform film thickness becomes flat at large time.

5 Conclusions

The flow and development of thin water-based CNTs nanoliquid film are investigated over a spinning horizontal disk. Using long wave singular perturbation technique, governing coupled nonlinear set of partial differential equations are solved analytically. The method of characteristics is used to solve the nonlinear film evolution equation. The following conclusions have been drawn from this study.

- The nanoliquid film thickness increases with higher values of CNTs volume fraction ϕ for both SWCNTs and MWCNTs.
- The film thinning rate diminishes with higher values of the Biot number Bi.
- The initial non-uniform film thickness becomes planar at large time.

Acknowledgements S. Maity expresses his sincere gratitude to the Council of Scientific and Industrial Research (CSIR), New Delhi, India, for the financial support with file number 25(0267)/17/EMR-II.

References

1. Emslie, A. C., Bonner, F. D., & Peck, L. G. (1958). *Journal of Applied Physics, 29*, 858–862.
2. Acrivos, A., Shah, M. J., & Petersen, E. E. (1960). *Journal of Applied Physics, 31*, 963–968.
3. Jenekhe, S. A., & Schuldt, S. B. (1984). *Industrial and Engineering Chemistry Fundamentals, 23*, 432–436.
4. Higgins, B. G. (1986). *Physics of Fluids, 29*, 3522–3529.
5. Myerhofer, D. J. (1978). *Journal of Applied Physics, 49*, 3993–3997.
6. Middleman, S. (1987). *Journal of Applied Physics, 62*, 2530–2532.
7. Dandapat, B. S., & Roy, P. C. (1994). *Journal of Physics D: Applied Physics, 27*, 2041–2045.
8. Dandapat, B. S., & Roy, P. C. (1993). *International Journal of Non-Linear Mechanics, 28*, 489–501.
9. Dandapat, B. S., & Singh, S. K. (2015). *Applied Mathematics and Computation, 258*, 545–555.
10. Dandapat, B. S., & Maity, S. (2009). *International Journal of Non-Linear Mechanics, 44*, 877–882.
11. Dandapat, B. S., Santra, B., & Kitamura, A. (2005). *Physics of Fluids*, *17*.
12. Choi, S. U. S., & Proc., (1995). *ASME International Mechanical Engineering Congress and Exposition, FED231/MD66* (pp. 99–105). ASME.
13. Buongiorno, J. (2006). *Journal of Heat Transfer, 128*, 240–250.
14. Akbar, N. S., & Butt, A. W. (2015). *Applied Mathematics and Computation, 259*, 231–241.
15. Hussanan, A., Khan, I., Gorji, M. R., & Khan, W. A. (2019). *Bio Nano Science, 9*, 21–29.
16. Maity, S. (2017). *International Nano Letters, 7*, 9–23.
17. Krishanan, R., Maity, S., Singh, S. K., Dandapat, B. S. (2020). *International Journal of Applied and Computational Mathematics*, *6*, 147(1–19).
18. Van Dyke, M. (1964). *Perturbation Methods in Fluid Mechanics*. Academic Pssress.